Journal of Medical Systems (2019) 43: 251
https://doi.org/10.1007/s10916-019-1356-8

IMAGE & SIGNAL PROCESSING

Improved Deep Learning Network Based in combination with Cost-sensitive Learning for Early Detection of Ovarian Cancer in Color Ultrasound Detecting System

Lei Zhang[1] · Jian Huang[1] · Li Liu[1]

Received: 7 March 2019 / Accepted: 22 May 2019 / Published online: 28 June 2019

Abstract
With the development of theories and technologies in medical imaging, most of the tumors can be detected in the early stage. However, the nature of ovarian cysts lacks accurate judgement, leading to that many patients with benign nodules still need Fine Needle Aspiration (FNA) biopsies or surgeries, increasing the physical pain and mental pressure of patients as well as unnecessary medical health care costs. Therefore, we present an image diagnosis system for classifying the ovarian cysts in color ultrasound images, which novelly applies the image features fused by both high-level features from deep learning network and low-level features from texture descriptor. Firstly, the ultrasound images are enhanced to improve the quality of training data set and the rotation invariant uniform local binary pattern (ULBP) features are extracted from each of the images as the low-level texture features. Then the high-level deep features extracted by the fine-tuned GoogLeNet neural network and the low-level ULBP features are normalized and cascaded as one fusion feature that can represent both the semantic context and the texture patterns distributed in the image. Finally, the fusion features are input to the Cost-sensitive Random Forest classifier to classify the images into "malignant" and "benign". The high-level features extracted by the deep neural network from the medical ultrasound image can reflect the visual features of the lesion region, while the low-level texture features can describe the edges, direction and distribution of intensities. Experimental results indicate that the combination of the two types of features can describe the differences between the lesion regions and other regions, and the differences between lesions regions of malignant and benign ovarian cysts.

Keywords Deep Learning · Ovarian cysts · Ultrasound detecting · Cost-sensitive Learning · Uniform local binary pattern · GoogLeNet

Introduction

Ovarian cancer is characterized by few early symptoms, presentation at an advanced stage, and poor survival [1]. As a result, it is the most frequent cause of death from gynecological cancer [2]. During the last decade, a research effort has been directed toward improving outcomes for ovarian cancer by screening for preclinical, early stage disease using both imaging techniques and serum markers. Numerous biomarkers have shown potential in samples from clinically diagnosed ovarian cancer patients, but there are still some missed detection, and marker detection is time-consuming and laborious [3]. Serum Carbohydrate Antigen 125 (CA125) has been widely applied in clinic because of its high sensitivity, but its accuracy is not high. The specificity of CA^{125} for early ovarian cancer is relatively low, so its application in large-scale ovarian cancer screening is limited. Imaging detection, such as Ultrasound, CT, Magnetic Resonance Imaging and Positron Emission Tomography (PET-CT) [4], play an important role in the localization and characterization of ovarian tumors [5]. But due to the recognition accuracy of the algorithm and the quality of ultrasonography, the specificity of ovarian cancer diagnosis is not very high. The combined detection of imaging and tumor

This article is part of the Topical Collection on *Image & Signal Processing*

✉ Li Liu
liliu_dsj10@163.com

[1] The Ultrasound Centre, Tianjin central hospital of gynecology obstetrics, Tianjin 300052, China

biomarkers can make up for their deficiencies [6, 7, 8]. In order to improve the accuracy of early ovarian cancer diagnosis, this paper proposes a tumor classification recognition algorithm for ovarian ultrasonography based on improved deep learning network, and carries out clinical verification combined with cancer biomarker diagnosis [9].

Existing studies on early diagnosis algorithms mainly focus on the extraction of manually designed features from the ovarian ultrasound images, and then the extracted features are supervised classification through the existing machine learning classifier. Chen et al. proposed to use genetic support vector machine to classify ovarian tumor by combining texture features with pathological features [10]; Chang et al. used wavelet coefficient, homogeneity, histogram and multi-scale gray difference as features to classify the ovarian ultrasound images to detect the types of tumor [11]. Katsigiannis et al. [12] used features based on image contour wavelet transform to classify ovarian ultrasonic texture; Acharya et al. used complex wavelet transform filter to extract features from 3D ultrasound images of ovaries to classify ovarian tumors [13]; Savelonas et al. proposed to use the features in random field to express the directional pattern in ovarian ultrasound images and supervised classifier to classify ovarian tumor [14]; Iacovidis et al. used a fuzzy local binary pattern (LBP) feature to classify and recognize the texture in ovarian ultrasound images. From the above analysis, we can see that most of the existing early diagnosis algorithms for ovarian cancer are to extract texture features directly from ultrasound images, and combine with support vector machine (SVM) classifier to complete the detection of cyst types [15]. In literature [16], Acharya et al. summarized the importance and advantages of ultrasonic image texture features for medical image classification. In this paper, the accuracy of medical image classification using non-medical features, such as tissue stiffness coefficient, texture and features based on discrete wavelet transform is significantly higher than that of medical features in images used alone, such as vascular distribution, edge void, and shape and micro-calcification points. However, traditional feature extraction requires the manual design of complex feature extraction methods [17, 18]. The extracted feature dimension is high, the workload is large and the efficiency is low.

A good knowledge of the underlying features in a data collection is required to extract the most relevant features [19]. This could become tedious and difficult when a huge collection of data needs to be handled efficiently. A major advantage of using deep learning methods is their inherent capability, which allows learning complex features directly from the raw data [20]. This allows us to define a system that does not rely on hand-crafted features, which are mostly required in other machine learning techniques. These properties have attracted attention for exploring the benefits of using deep learning in medical image analysis. The future of medical applications can benefit from the recent advances in deep learning techniques. There are multiple deep learning open source platforms available such as *Caffe, Tensorflow, Theano, Keras* and *Torch* [21]. The challenges arise due to limited clinical knowledge of deep learning experts and limited deep learning knowledge of clinical experts. A recent tutorial attempts to bridge this gap by providing a step by step implementation detail of applying deep learning to digital pathology images.

With the development of machine learning, deep learning has become a hot topic in the field of object recognition in recent years. Image features extracted by deep convolutional neural network (DCNN) [22, 23] are proved to be effective in image classification, segmentation or retrieval. As a kind of multi-layer neural network learning algorithm, deep learning technology can learn features through non-linear network structure, and form more abstract deep representation or features by combining low-level features to realize complex function approximation and to represent the distributed representation of the input data, which can effectively learn the essential characteristics of the data set [6]. Therefore, the application of deep learning algorithm in multi-modal medicine image aided diagnosis system has the following advantages: firstly, as a data-driven automatic feature learning algorithm, it can extract features directly from training data, thus greatly reducing the workload of feature extraction and the impact of manual feature; secondly, it can represent the intersection of features through the deep structure of neural network. Thirdly, the three core steps of feature extraction, feature selection and feature classification can be realized in the optimization of the same deep structure. Thus, deep learning is expected to solve the problem of insufficient ability based on traditional shallow machine learning, thus greatly improving the ability of assistant diagnosis. Existing research results show that DCNN algorithm is not affected by interference and has good robustness, compared with the traditional feature extraction algorithm.

Based on the advantages of DCNN in non-medical images, DCNN has been gradually applied to medical image classification and detection. Spanhol et al. proposed to use DCNN to classify ovarian cancer pathological images [24]; Li et al. proposed a classification system of pulmonary nodules based on DCNN [25]; Roth et al. proposed an algorithm for developing a lymph node detection system using DCNN [22]. Based on the successful experience of DCNN in medical image, this paper attempts to use DCNN to classify tumor in ovarian ultrasound images, so as to realize the early diagnosis of tumors. However, there is no uniform standard for the images used to train the DCNN model at present, and a large number of wrong labels exist in benchmark data. The data amount of the training image is still small, which is not enough to train the convolutional neural network independently. Therefore, in order to improve the accuracy of early diagnosis, this paper proposes an improved convolutional neural network. The

network uses fine-tuning parameters to extract the deep features of images, and fuses the deep features with texture features. Finally, the features are input into Cost-sensitive Random Forest classifier to classify the benign and malignant ovarian tumor.

Related Works

Convolutional Neural Network

Convolution neural network (CNN) is a multi-layer perceptron with autonomous supervised learning [20, 26, 27]. It mainly includes input layer, hidden layer (convolutional layer and down-sampling layer) and output layer. It updates network parameters by reverse conduction optimization network. In the convolutional layer, multiple feature maps will be obtained. Each feature map extracts one feature. Each neuron of the feature image is connected with the local receptive field of the previous layer and shares a set of weights. Through convolution operation, the process of feature extraction is completed. Since multiple feature maps have multiple different weights, different features can be obtained. In the process of training, the weights are constantly updated by reverse conduction, so that the final classification results develop towards a more accurate direction. The formula for calculating the convolutional layer is:

$$x_j^l = f\left(\sum_{i \in M_j} x_i^{l-1} k_{i,j}^l + b_j^l\right) \tag{1}$$

where M_j is the set of all input maps; K_{ij} is convolutional kernel; $b_j$is the offset of each input map.

The purpose of the down-sampling layer is to realize the pooling effect of the feature map, so as to reduce the resolution of the image and keep the number of the feature map unchanged. In addition to the reduction of feature dimension, the robustness to displacement, scaling and distortion is also enhanced to some extent. The down-sampling formula is:

$$x_j^l = f\left(\beta_j^l d\left(x_j^{l-1}\right) + b_j^l\right) \tag{2}$$

where d represents a down-sampling function; β_j is weight coefficient.

In order to extract the non-linear deep features, the convolution feature image is extracted using the three-layer micro-network structure shown in Fig. 1. Assuming that a small area with the size$r_1 \times r_2$is extracted from the starting coordinate and is successively labeled as (1, 1),(1, 2),....,$(b_1 - r_1 + 1, b_2 - r_2 + 1)$, the extracted regions are convoluted with the feature base feature $\varphi_1, \varphi_2, \cdots, \varphi_{m1}$of the trained sparse self-encoder one by one. The m_1 data corresponding to each patch constitute the input of a sub-SAE network, which is stacked in three layers. After convolution operation, the$m_1$global feature image with the size$(b_1 - 3r_1 + 3, b_2 - 3r_2 + 3)$is obtained.

GoogLeNet Model

In the existingt mainstream DCNN model, GoogLeNet has proved to be a good classifier for images [28]. GoogLeNet is the ILSVRC classification champion in 2014 [8]. GoogLeNet is a 22-layer convolutional neural network, which innovatively proposes the structure of "perception layer". The "perception layer" can be regarded as a combination of a set of "network-in-network" filters and convolution filters of different sizes between layers. Each "network-in-network" filter is connected to a 3×3 or 5×5 pixel filter, which is then fed into the pooling layer and the connection layer, as shown in Fig. 2. Each layer has filters of different sizes to correspond to the input features with different resolution in that layer. One of the main beneficial aspects of this architecture is that it allows for increasing the number of units at each stage significantly without an uncontrolled blow-up in computational complexity. The

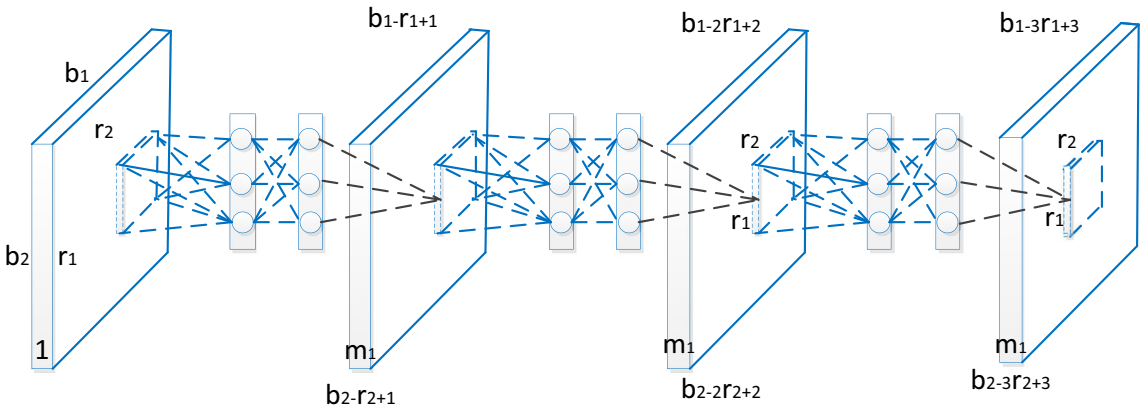

Fig. 1 Convolution feature image with three-layer single-block network structure

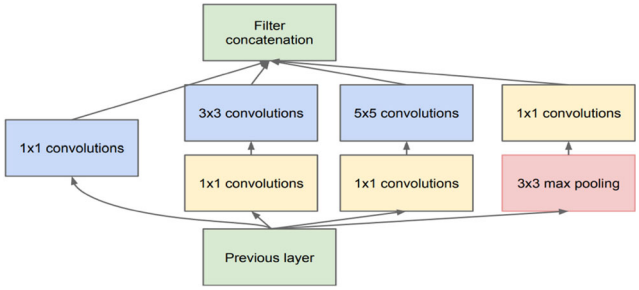

Fig. 2 Inception module with dimension reduction

ubiquitous use of dimension reduction allows for shielding the large number of input filters of the last stage to the next layer, first reducing their dimension before convolving over them with a large patch size. Another practically useful aspect of this design is that it aligns with the intuition that visual information should be processed at various scales and then aggregated so that the next stage can abstract features from different scales simultaneously [29]. The improved use of computational resources allows for increasing both the width of each stage as well as the number of stages without getting into computational difficulties. Another way to utilize the inception architecture is to create slightly inferior, but computationally cheaper versions of it. The model have found that all of strategies allow for a controlled balancing of computational resources that can result in networks that are two times faster than similarly performing networks with non-Inception architecture, however this requires careful manual design at this point.

Although GoogLeNet is very deep, its parameters are 12 times less than AlexNet, so the calculation of training is more efficient. Although the recognition of natural images by GoogLeNet is excellent, the direct application of the network to the ultrasound ovarian cyst images will result that the network cannot converge because of the great difference between the content of the image and the original training sample, and cannot get a good classification and recognition effect. Therefore, we need to adopt the transfer learning method to input the pre-processed ultrasound image samples into the pre-trained GoogLeNet for parameter fine-tuning, so as to make it more sensitive to the ovarian image. Then the fine-tuned network is used to extract the features of ovarian cancer image. Finally, the extracted high-level deep features and low-level texture features are fused for image classification and recognition.

GoogLeNet has a deeper network structure and fewer parameters and computational complexity, mainly due to the extensive use of 1×1 convolution in convolution network and the replacement of full connection layer in traditional network architecture with average pool. Of course, this requires careful design of Inception Architecture so as to achieve the final excellent results.

The Proposed Early Diagnosis Algorithm of Ovarian Cyst

Data Extension

The original GoogLeNet network was trained on the *mnist* data set, which was not highly sensitive to the ovarian cyst images [30]. However, the existing ovarian image data is not enough to train a new network, so the existing images are used for transfer learning and parameter fine-tuning of trained GoogLeNet to obtain the deep network sensitive to ovarian image features.

Due to the limited sample size of the existing data set, we need to expand each sample. At present, the mainstream methods of image sample expansion mainly include Angle Rotation, Scale Transformation and Contrast Transformation, which are not suitable for medical image expansion. Therefore, a new data expansion method is proposed in this paper. Firstly, the location of the label given by the radiologists for the location of the ovarian cyst is calculated; then, the coordinates(x_t, y_t),(x_l, y_l), (x_b, y_b),(x_r, y_r) of the four boundaries of the ovarian cyst area are calculated according to the location of the label; finally, with the cyst area as the center, 9 image parts including both the cyst area and its surrounding tissue area were taken as the expanded samples. Taking the upper left area as an example, the coordinate area of the expanded sample$W \times W$in the image$m \times n$can be expressed as:

$$\mathrm{I}_1 : I\begin{pmatrix} \max(x_l - W/2, 1) : \min(x_l + W/2, m), \\ \max(y_t - W/2, 1) : \min(y_t + W/2, n) \end{pmatrix} \tag{3}$$

where W represents the width of the target area; $x_l$and$y_t$are the abscissa and ordinate of the left label and the upper label, respectively. The coordinates of the other eight areas can be calculated in the similar way.

By using this method to expand the original image samples, the simulation results show that each extended sample contains both suspected lesion area and surrounding tissue area, so that DCNN can better learn the features of ovarian cyst from the texture of nodule tissue itself and the difference between cyst tissue and other tissues.

Deep Feature Extraction Based on Transfer Learning

After the expanded training image samples are obtained, it can fine-tune the parameters of GoogLeNet to obtain a deep network that can accurately learn and extract the features in the ovarian ultrasound images. Caffe deep learning framework is adopted in this paper to fine-tune the GoogLeNet network. In supervised learning, objective function (Loss function) is used to evaluate the consistency between the output value and the real value of input samples after model discrimination. The

commonly used loss functions are Squared Loss Function, Cross-Entropy Loss Function and Softmax Loss Function. This paper intends to use Softmax Loss function. Considering that it is more difficult to collect cyst samples than health samples in the practical application of ovarian cyst diagnosis, and there will be extremely unbalanced data sets, so that the weight loss functionW_s shown in formula (4) is introduced to give smaller weights to the types with larger quantities and larger weights to the types with smaller quantities. At the same time, the L2 regularization penalty term as shown in formula (5) is added to improve the poor generalization ability of the model caused by the sample imbalance problem. The regular term and the cross-entropy function are merged into the weight loss function shown in formula (6)

$$W_s = -\frac{1}{Q}\sum_{q=1}^{Q}\sum_{c=1}^{C} v_c I\{y^q = c\}\log\left(P_c^{(q)}\right) \tag{4}$$

$$v_c = \frac{\max\{n_c\}_{c=1}^{C}}{n_c} \tag{5}$$

$$n_c = \sum_{q=1}^{Q} I\{y^q = c\} \tag{6}$$

$$P_c^{(q)} = \frac{\exp\left(\left(w_c^{K,l}\right)^T x^{(q),L-1}\right)}{\sum_{c=1}^{C}\exp\left(\left(w_c^{K,l}\right)^T x^{(q),L-1}\right)} \tag{7}$$

$$R(W) = \sum_K \sum_l W_{K,l}^2 \tag{8}$$

$$L = W_s + \lambda R(W) \tag{9}$$

n_c represents the number of class c samples in formula(4); v_c represents the degree of imbalance between class c samples and other samples; $C$and$Q$represent the total classes and total samples, respectively; $P_c^{(q)}$ represents the output value of the input sample through Softmax function; $w_c^{K,l}$ denotes connection weight; $y^q$is the class label of sample$y$ under class q;T is the transpose of the matrix; L is the number of deep network layers; λin formula (6) is the penalty coefficient of the regular term; R(W) in formula(8) is the weight matrix of deviation term.

Classification of Ovarian Ultrasound Images by Fusing Deep Features and Shallow Texture

Deep neural network can classify images directly, but it does not take advantage of the low-level features of images [31]. Considering that there are a large number of low-level features such as texture in medical images, this paper uses deep neural network to extract deep features from images and fuse them with texture features, and then uses cost sensitive classifier to classify images.

The rotation invariant local binary pattern (ULBP) can be used as a shallow feature to accurately describe texture features in ultrasound images. For any pixel(x, y) in an image, its LBP coding follows the definition of

$$\mathrm{B}_{P,R}(x_c, y_c) = \sum_{p=0}^{P} S\left(n_p - n_c\right)2^p \tag{10}$$

whereS()is defined as follows:

$$\mathrm{S}(x) = \begin{cases} 1, & |x| \geq T_{LBP} \\ 0, & |x| < T_{LBP} \end{cases} \tag{11}$$

where n_c is the pixel value for neighborhood center point(x_c, y_c);$n_p$is the pixel value of the p-th pixel point on the circle with the center point as the center and the radius as R; $T_{LBP}$is a small positive value to enhance the robustness of LBP for the description of smooth regions in the image.

After obtaining the LBP code of arbitrary pixels, the LBP translation code with the minimum value can be obtained by cyclic right displacement, and then the local binary pattern with rotation invariance can be obtained. The above calculation for all points are done in the image, and the histogram of the translated value of the local binary pattern is counted as the shallow texture feature of the image.

Given an ultrasound image of ovarian cyst to be classified, input it into the fine-tuned GoogLeNet. The output of the network is the deep feature of the image, and the dimension of the deep feature is 1024. For the shallow texture feature of image, ULBP is adopted as the texture feature of image. The dimension of the ULBP feature is 59. The two features are normalized and then cascaded to obtain the high and low level fusion features of the image.

$$\overline{F}_h = \frac{F_h - F_h^{\min}}{F_h^{\max} - F_h^{\min}} \tag{12}$$

$$\overline{F}_l = \frac{F_l - F_l^{\min}}{F_l^{\max} - F_l^{\min}} \tag{13}$$

$$F = \left\{\overline{F}_h, \overline{F}_l\right\} \tag{14}$$

where $\overline{F}_h$ is the normalized deep featureF_h;$F_h^{\max}$, $F_h^{\min}$ respectively are minimum and maximum of non- normalized deep feature sector; $\overline{F}_l$, F_l, $F_l^{\max}$, $F_l^{\min}$ respectively are normalized value, non-normalized value of texture feature, minimum and maximum of non-normalized feature vector; F represents the joint feature combining depth feature and texture feature for image classification.

Ovarian Ultrasound Image Classification Based on Cost-Sensitive Random Forest Classifier

Because the benign and malignant cases of ovarian cyst images are not balanced, this paper adopts the cost-sensitive random forest algorithm to classify the images.

In view of the benign and malignant classification of ovarian tumor in this paper, it is assumed that malignant

(+ or + 1) represents minority class and benign (− or − 1} represents majority class. A case should belong to class$j$, but the cost of being misclassified as class i is$C(i,j)$. The cost sensitive classification model is established to minimize the non-classification cost:

$$H(x,y) = \arg\min_{i,j} \sum (P(j|x)C(i,j) + P(i|y)C(j,i)) \quad (15)$$

where P(j, x)and$P(i|$ y)are the posterior probability of classifying case$x$to class$j$ and classifying case$y$ to class$i$. Then, the above cost factors are introduced into the random forest to deal with unbalanced data classification. The algorithm steps are given as follows:

1. Bootstrap data set is acquired through Bagging method
2. Establish a non-pruning classification regression (CART) decision tree for each Bootstrap data set, and introduce cost factor into Gini index calculation of CART decision tree.

$$I_C(t) = \sum_{i,j} C_{ij} p(i/t) p(j/t) \quad (16)$$

where C_{ij}denotes the misclassified cost. In practical application, the cost sensitive random forest classification algorithm is realized by using WEKA data analysis environment, which only needs to determine the decision-making, the number of trees and cost-sensitive matrix.

Experimental Results and Analysis

In this Section, we will compare and validate the effectiveness of our proposed ultrasound image classification system based on the fusion of deep feature and texture features for ovarian cysts.

Experimental Data

Ultrasound images of ovarian cysts are obtained from an open source database provided by Pedraza et al. [32]. The database consists of 428 ultrasound images with the size 560×360 pixels, where 357 are malignant and 71 are benign tumor. At the same time, we also built 1400 ovarian ultrasound samples form Peking Union Medical College Hospital, where 277 are ovarian cancer samples, 299 are benign cyst samples, and the rest are normal ovarian ultrasound images. The images are extracted from the ovarian ultrasound video sequences collected at 12 MHz by TOSHIBA Nemio 30 and TOSHIBA Nemio MX ultrasound instruments. In addition, the database contains most of the pathological features and pathological diagnosis obtained by biopsy and BETHESDA system, and the diagnosis results are independently confirmed by professional doctors. As shown in Table 1, 1628 ovarian ultrasound images from different case are randomly grouped and expanded seven times. Each grouping ensured that 806 of them are used to train GoogLeNet, 420 images are used to validate GoogLeNet model, and the remaining sample images are used as test data sets.

Table 1 The distribution of training, validating and testing samples in data-set (one group)

	Total		malignant		Benign	
	Cases	Samples	Cases	Samples	Cases	Samples
Training	306	2745	256	2340	50	452
Validating	61	549	51	459	10	101
Testing	61	549	50	450	11	99

Experimental Steps and Evaluation Criteria

In order to analyze fairly the performance of the deep-based learning algorithm for ovarian cyst image classification, l0-fold cross validation [33] is used to calculate the relevant evaluation indicators and compare with other algorithms. In the same data set, the current mainstream ovarian cyst image classification algorithms are compared, and the performance of each algorithm on other data sets (non-open source) is also compared, where the comparison algorithms are Fully Connected Convolutional Neural Network (FCNN) [34], Five-Layer Convolutional Neural Network (CNN) [35], AlexNet [36], VGNet and GoogLeNet and their parameters are set to official defaults [25, 26, 32].

For cost-sensitive random forest classifiers, we set the number of decision trees to 10, and the cost matrix is determined by the proportion of benign and malignant cases in the data set. For the classification results, the accuracy (ACC), sensitivity (SENS), specificity (SPEC) and the area under ROC curve are used to evaluate the classification results. The specific definitions are written as follows.

$$ACC = \frac{TP + TN}{TP + FP + FN + TN} \quad (17)$$

$$SENS = \frac{TP}{TP + FN} \quad (18)$$

$$SPEC = \frac{TN}{TN + FP} \quad (19)$$

In these formulas, ACC, SENS and SPEC indicate the accuracy, sensitivity and specificity, respectively; TP, TN, FP and FN are indicated as the number of true positive, true negative, false positive and false negative, respectively.

Classification Results for Given Data Sets

This experiment carries out 10-fold cross validation on different algorithms, obtains the experimental results and calculates their indicators. Finally, the average values of six groups of indicators are obtained, which is the classification accuracy, sensitivity, specificity and the area under the ROC curve of the proposed classification algorithm for the test data set. Table 2 shows the classification accuracy, sensitivity, specificity and the area under the maximum ROC curve of the proposed algorithm and other algorithms, while Fig. 3 shows the corresponding ROC curve. The classification accuracy, sensitivity, specificity and ROC area of the proposed algorithm are 99.15%, 99.70%, 95.85% and 0.997 respectively. The ROC curve is closer to the upper left corner of the region. It shows that the proposed algorithm can guarantee high sensitivity and specificity, and can accurately distinguish benign and malignant cysts.

Comparison for Existing Classification Algorithms of Ovarian Cysts

Although other data sets for evaluating ovarian cyst image classification algorithms are not open source, their accuracy can still be used as a reference to evaluate the proposed algorithm. It can be seen that the algorithm proposed in this paper firstly classifies the ovarian cyst image using deep learning method, and the accuracy is higher than other algorithms. Although it can not be directly compared with other algorithm models, it can reflect that the proposed algorithm based on deep learning can more accurately assess the risk of can creation of ovarian ultrasound images on larger data sets.

The improved network training loss curve and verification accuracy are shown in Fig. 4. The abscissa represents the number of iterations, while the ordinate represents the loss value in the training process and the accuracy in the verification process. With the increase of training iterations, the training loss decreases significantly, and the verification accuracy increases accordingly. The training LOSS converges about

Table 2 Comparison of the effects of classifying testing data by different methods (same data}et)

Algorithms	ACC(%)	SENS(%)	SPEC(%)	AUC(%)
VGNet	97.12	97.36	92.18	0.982
AlexNet	98.29	99.10	93.9	0.995
FCNN	93.08	93.85	91.15	0.962
CNN	92.06	92.13	84.56	0.941
GoogLeNet	96.68	96.78	92.84	0.975
Proposed	99.15	99.73	95.85	0.997

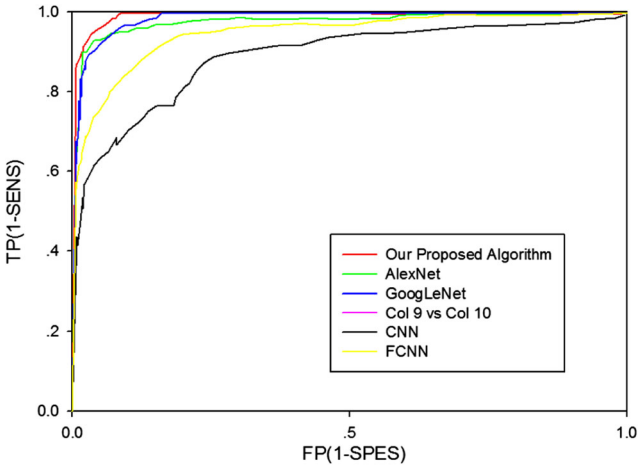

Fig. 3 The ROC curves of applying different classification methods to classify images in the testing data-set

1000 times and the accuracy of verification set in the training process reaches about 88%.

In this paper, a new classification algorithm based on deep convolution neural network is proposed for ovarian ultrasound images. The image is preprocessed to improve the quality of training image. The existing GoogLeNet network is migrated and learned by using high-quality training images. The deep features obtained by deep network and image texture features are fused to obtain stroger features. A cost-sensitive random forest classifier is used to classify the unbalanced distribution of data sets. The experimental results show that the proposed algorithm can effectively improve the accuracy of classification of ovarian cyst ultrasound images, reduce the probability of misclassification, and is more in line with the assessment of ovarian cyst canceration risk by ultrasound imaging experts.

Clinical Diagnosis Based on our Proposed Recognition Algorithm in Combination of Tumor Markers Detection

Ultrasound can continuously, dynamically and real-time observe the movement function of organs, display the three-dimensional changes of the lesion, and Doppler angiography can observe the flow and direction of the blood flow of the lesion. Ultrasound equipment is flexible and can be used for bedside diagnosis of severe patients. It is cheap, radiation-free, safe and non-invasive. Ultrasound is the best method to detect benign and malignant ovarian lesions. At present, transvaginal ultrasound, transabdominal ultrasound and color Doppler flow imaging are widely used. The accuracy of transabdominal ultrasonography in detecting ovarian cancer, especially serous ovarian cancer, is higher than that of CT. However, the imaging quality is affected by many factors, such as body shape, subcutaneous fat thickness, ascites, depth of mass, etc. It is easy to be confused with intestinal cavity,

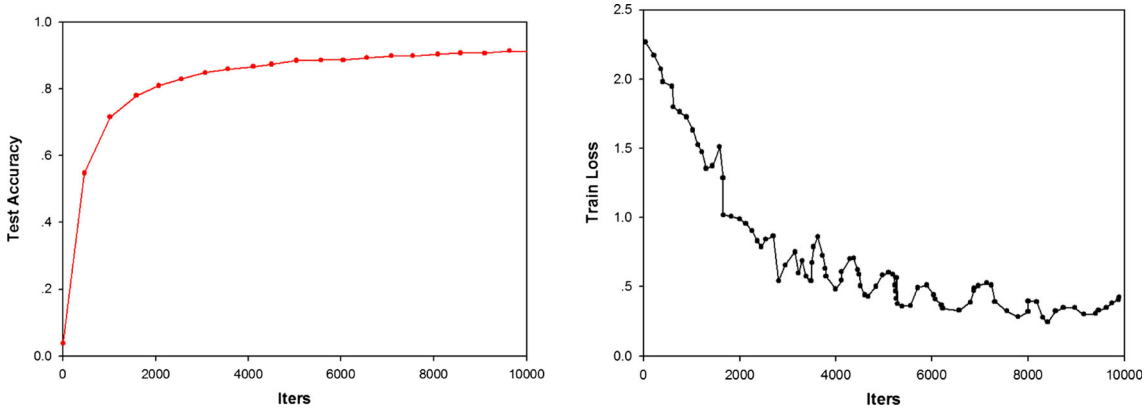

(a) The verified accuracy of transfer learning (b) The loss function curve of our improved algorithm

Fig. 4 Performance Curves (a) The verified accuracy of transfer learning (b) The loss function curve of our improved algorithm

which increases the probability of missed diagnosis. The improved depth learning algorithm proposed in this paper can increase the recognition accuracy, but if the imaging quality is not satisfactory, the algorithm in this paper can not help. Therefore, in view of the clinical reality, this paper proposes to use the detection of tumor markers as an auxiliary, and use it in conjunction with the algorithm, so as to improve the accuracy of diagnosis. Ultrasound combined with serum tumor markers is easier to be popularized in clinic because it is cheaper than CT and MRI. In clinical trials, CA125 and carbohydrate antigen 19-9(CA19-9) were used as markers to synthetically analyze and judge 180 patients with ovarian cancer. The results showed that the sensitivity and specificity of combined detection for predicting ovarian malignant tumors were improved. The combined detection was easy to implement, non-invasive and inexpensive, and could be used in the screening and diagnosis of ovarian malignant tumors. It is worth popularizing and applying in clinic.

Conclusions

With the development of theories and technologies in medical imaging, most of the tumor can be incidentally detected in the early stage. However, the nature of ovarian cysts lacks accurate judgement, leading to that many patients with benign nodules still need Fine Needle Aspiration (FNA) biopsies or surgeries, increasing the physical pain and mental pressure of patients as well as unnecessary medical health care costs. Therefore, we present an image diagnosis system for classifying the ovarian cysts in color ultrasound images. Firstly, the ultrasound images are augmented to enlarge the size of training data set and used to fine-tune the parameters of the pretrained GoogLeNet convolutional neural network, and the rotation invariant uniform local binary pattern (ULBP) features are extracted from each of the images as the low-level texture features. Then the high-level deep features extracted by the fine-tuned GoogLeNet neural network and the low-level ULBP features are normalized and cascaded as one fusion feature that can represent both the semantic context and the texture patterns distributed in the image. Finally, the fusion features of the images are sent to the Cost-sensitive Random Forest classifier to classify the images into “malignant” and”benign”. Experimental results indicate that the high-level features extracted by the deep neural network from the medical ultrasound image can characterize the visual features of the lesion region, while the low-level texture features can describe the edges, direction and distribution of intensities. The combination of the two types of features can describe the differences between the lesion regions and other regions, and the dilferences between lesions regions of malignant and benign ovarian cysts. In addition, our proposed algorithm also has scale problem, which we will solve in future.

Compliance with ethical standards

Conflict of interest We declare that we have no conflict of interest.

Human and Animal Rights This article does not contain any studies with human participants or animals performed by any of the authors.

Informed consent Informed consent was obtained from all individual participants included in the study.

References

1. Sadowski, E. A. et al., A systematic approach to adnexal masses discovered on ultrasound: the ADNEx MR scoring system. Abdominal Radiology 43(3):679–695, 2018.
2. Faust, O. et al., Comparative assessment of texture features for the identification of cancer in ultrasound images: a review. Biocybernetics and Biomedical Engineering 38(2):275–296, 2018.
3. Perera, R. et al., Ultrasound contrast agents and delivery systems in cancer detection and therapy. Advances in Cancer Research 139. Academic Press:57–84, 2018.

4. Lusk, J. F., et al. Photoacoustic Flow System for the Detection of Ovarian Circulating Tumor Cells Utilizing Copper Sulfide Nanoparticles. ACS Biomaterials Science & Engineering, (2019).
5. Kam, H. J., Kim, H. Y., Learning representations for the early detection of sepsis with deep neural networks[J]. Computers in Biology and Medicine, S0010482517302743, 2017.
6. Luo, B., Wang, H., Liu, H., et al. Early Fault Detection of Machine Tools Based on Deep Learning and Dynamic Identification[J]. IEEE Transactions on Industrial Electronics, PP(99):1-1, (2018).
7. Ghatwary, N., Zolgharni, M., Ye, X., Early esophageal adenocarcinoma detection using deep learning methods[J]. International Journal of Computer Assisted Radiology and Surgery, (3):1-11, (2019).
8. Lee, Y.-B., Choi, Y.-J., and Kim, M.-H., Boundary detection in carotid ultrasound images using dynamic programming and a directional Haar-like filter. Comput. Biol. Med. 40(8):687–697, 2010.
9. Menchón-Lara, R-M., Sancho-Gómez, J-L., Bueno-Crespo, A., Early-stage atherosclerosis detection using deep learning over carotid ultrasound images[M]. Elsevier Science Publishers B. V. (2016).
10. Chen, S. J., Chang, C. Y., Chang, K. Y. et al., Classification of the thyroid nodules based on characteristic sonographic textural feature and correlated histopathology using hierarchical support vector Machines[J]. Ultrasound in Medicine and Biology 36(12):2018–2026, 2010.
11. Chang, C. Y., Liu, H. Y., Tseng, C. H. et al., Computer-aided diagnosis for thyroid graves'disease in ultrasound images[J]. Biomedical Engineering: Applications, Basis and Communications 22(2):91–99, 2010.
12. Katsigiannis, S., Keramidas, E. G., and Maroulis, D., A contourlet transform feature extraction scheme for ultrasound thyroid texture classification[J]. International Journal of Engineering Intelligent Systems for Electrical Engineering and Communications 18(3-4): 171, 2010.
13. Acharya, U. R., Sree, S. V., Swapna, G. et al., Effect of complex wavelet transform filter on thyroid tumor classification in three-dimensional ultrasound[J]. Proceedings of the Institution of Mechanical Engineers, Part H: Journal of Engineering in Medicine 227(3):284–292, 2013.
14. Iakovidis, D. K., Keramidas, E. G., Maroulis, D., Fuzzy local binary patterns for ultrasound texture characterization[C]//Proceedings of the 5th International Conference on Image Analysis and Recognition. Póvoa de Varzim, Portugal: Springer, 750-759, (2008).
15. Chang, C. Y., Chen, S. J., and Tsai, M. F., Application of support-vectormachine-based method for feature selection and classification of thyroid nodules in ultrasound images[J]. Pattern Recognition 43(10):3494–3506, 2010.
16. Acharya, U. R., Swapna, G., Sree, S. V. et al., A review on ultrasoundbased thyroid cancer tissue characterization and automated classification[J]. Technology in Cancer Research and Treatment 13(4):289–301, 2014.
17. Ma, S., Sigal, L., Sclaroff, S., Learning Activity Progression in LSTMs for Activity Detection and Early Detection[C]// 2016 IEEE Conference on Computer Vision and Pattern Recognition (CVPR). IEEE, (2016).
18. Costa, A. C., Oliveira, H. C. R., Catani, J. H., et al. Data Augmentation for Detection of Architectural Distortion in Digital Mammography using Deep Learning Approach[J]. (2018).
19. Aliamiri, A., Shen, Y., Deep learning based atrial fibrillation detection using wearable photoplethysmography sensor[C]// IEEE Embs International Conference on Biomedical & Health Informatics. IEEE, 442-445, (2018).
20. Liang, Q., Wendelhag, I., Wikstrand, J., and Gustavsson, T., A multiscale dynamic programming procedure for boundary detection in ultrasonic artery images. IEEE Trans. Med. Imaging 19(2):127–142, 2000.
21. Krizhevsky, A., Sutskever, I., Hinton, G. E., ImageNet classification with deep convolutional neural networks[C]//Proceedings of the 25th International Conference on Neural Information Processing Systems. Lake Tahoe, Nevada: Curran Associates Inc., 1097-1105, (2012)
22. Roth, R. H., Lu, L., Seff, A., et al. A new 2. 5D representation for lymph node detection using random sets of deep convolutional neural network observations[C]//Proceedings of the 17th International Conference on Medical Image Computing and ComputerAssisted Intervention. Boston, MA, USA: Springer, 520-527, (2014).
23. Menchón-Lara, R-M., Sancho-Gómez, J-L., Bueno-Crespo, A., Early-stage atherosclerosis detection using deep learning over carotid ultrasound images[J]. Applied Soft Computing, S1568494616304574, (2016).
24. Spanhol, F. A., Oliveira, L. S., Petitjean, C., et al. Breast cancer histopathological image classification using convolutional neural networks[C]//Proceedings of 2016 International Joint Conference on Neural Networks. Vancouver, BC, Canada: IEEE, 2560-2567, (2016).
25. Li, W., Cao, P., Zhao, D. Z., et al. Pulmonary nodule classification with deep convolutional neural networks on computed tomography images[J]. Computational and Mathematical Methods in Medicine, 2016: #6215085, (2016).
26. Bengio, Y., Courville, A., and Vincent, P., Representation learning: a review and new perspectives. IEEE Trans. Pattern Anal. Mach. Intell. 35(8):1798–1828, 2013. https://doi.org/10.1109/TPAMI.2013.50.
27. Loizou, C. P., Pattichis, C. S., Pantziaris, M., Tyllis, T., and Nicolaides, A., Snakes based segmentation of the common carotid artery intima media. Med. Biol. Eng. Comput. 45(1):35–49, 2007.
28. Cheng, D.-C., and Jiang, X., Detections of arterial wall in sonographic artery images using dual dynamic programming. IEEE Trans. Inf. Technol. Biomed. 12(6):792–799, 2008.
29. Xu, X., Zhou, Y., Cheng, X., Song, E., and Li, G., Ultrasound intima-media segmentation using though transform and dual snake model. Comput. Med. Imaging Graph. 36(3):248–258, 2012.
30. Huang, G.-B., Zhu, Q.-Y., and Siew, C.-K., Extreme learning machine: theory and applications. Neurocomputing 70(1–3):489–501, 2006. https://doi.org/10.1016/j.neucom.2005.12.126.
31. Deng, L., Yu, D. Deep learning: methods and applications[J]. Foundations & Trends in Signal Processing, 2014, 7(3):197–387.
32. Kasun, L. L. C., Zhou, H., Huang, G.-B., and Vong, C. M., Representational learning with extreme learning machine for big data. IEEE Intell. Syst. 28(6):31–34, 2013.
33. W. Zong, G. B. Huang, Y. Chen, Weighted extreme learning machine for imbalance learning, Neurocomputing 1:24.
34. Santhiyakumari, N., and Madheswaran, M., Non-invasive evaluation of carotid artery wall thickness using improved dynamic programming technique. Signal Image Video Process. 2(2):183–193, 2008.
35. Huang, G.-B., Zhou, H., Ding, X., and Zhang, R., Extreme learning machine for regression and multiclass classification. IEEE Trans. Syst. Man Cybern. Part B: Cybern. 42(2):513–529, 2012. https://doi.org/10.1109/TSMCB.2011.2168604.
36. Molinari, F., Meiburger, K. M., Saba, L., Acharya, U. R., Ledda, M., Nicolaides, A., and Suri, J. S., Constrained snake vs. conventional snake for carotid ultrasound automated IMT measurements on multi-center data sets. Ultrasonics 52(7):949–961, 2012.